# Stationary High-Field Domains in the Range of Negative Differential Conductivity in CdS Single Crystals*

K. W. Böer and P. Voss

*Physics Department, University of Delaware, Newark, Delaware*

(Received 30 October 1967)

In CdS crystals with an $N$-shaped negative differential conductivity range, stationary high-field domains adjacent to the electrodes are observed. With increasing applied voltage these steplike domains increase in width, staying attached to the cathode until they fill the entire crystal; then a still higher-field domain forms at the anode and increases in width. These domains can be explained within an earlier published theory, and allow the determination of electron densities at the cathode-CdS boundary and in the field-quenched region. The analysis of these stationary domains presents a new tool for work-function (metal-semiconductor) investigations.

## 1. INTRODUCTION

IN crystals having a negative differential conductivity range at high electric fields, typical high-field domains occur at high enough applied voltages, which, under certain conditions, e.g., those attainable by proper doping, do not move. These high-field domains lie adjacent to the electrodes, have a steplike shape, and have been observed, using direct field probing with the Franz-Keldysh effect[1] and conventional potential probing[2] in CdS. It is assumed that these stationary domains are a preceding form of the well-known moving domains[1,3–10] which are accompanied by current oscillations, and that these stationary domains will occur only for a certain range of average fields, or when hindered in motion through the crystal by some crystal faults.[5]

In this paper evidence will be given that, even up to voltages corresponding to averaged fields well above the negative differential conductivity range, these stationary field domains can be stable in some CdS crystals, and that it is very improbable that this stability is caused by a hindered motion due to crystal faults or unfavorable electrode geometry.

It will be shown that these stationary high-field domains can be understood in the light of an earlier published theory,[5,11,12] and give information on the carrier densities at the metal-semiconductor boundary and in the bulk of the crystal for zero space charge.

## 2. EXPERIMENTAL METHOD

CdS single-crystal platelets grown at about 1000°C by sublimation of high-purity CdS powder in an atmosphere of $N_2$ and $H_2S$ were used. These platelets were doped by heating in an $H_2S$ atmosphere at about 900°C for 3 h, in a bed of CdS powder containing a given amount of Cu or Ag and Al nitrates. The crystals were high resistive. The central part of the crystal, used for later investigation, was protected from direct contact with the CdS powder, and was cleaved from the platelet. Gold electrodes were evaporated onto the side edges of the crystal (crystal dimensions, $0.1 \times 0.36 \times 0.57$ mm³). The crystals were held on a Cu crystal holder at a temperature of $-65$°C. For analysis of the field distribution using the Franz-Keldysh effect, photos of the CdS platelets were taken in monochromatic light close to the absorption edge, revealing high-field domains as dark layers in the crystal (layers of increased optical absorption).

The current through the crystal and the voltage drop between the electrodes were measured with an $X$-$Y$ recorder.

## 3. THEORY OF STATIONARY HIGH-FIELD DOMAINS IN CdS

The time-independent Poisson and transport equations

$$dE/dx = (e/\epsilon\epsilon_0)\rho(x),$$
$$dn/dx = (1/\mu kT)(e\mu nE - j), \tag{1}$$

for an $n$-type photoconductor model containing, e.g., field quenching as a mechanism to produce a negative differential conductivity range, have steplike solutions

* Supported by the U. S. Office of Naval Research under Contract No. NONR (G) 4336-(00).

[1] K. W. Böer, H. J. Hänsch, and U. Kümmel, Z.Physik 155, 460 (1959); W. Franz, Z. Naturforsch. 13a, 484 (1958); I. V. Keldysh, Zh. Eksperim. i Teor. Fiz. 34, 1138 (1958) [English transl.: Soviet Phys.—JETP 6, 788 (1958)].

[2] H. Kiess, Phys. Status Solidi 4, 107 (1964).

[3] W. Shockley, Bell System Tech. J. 33, 799 (1954).

[4] K. W. Böer, *Festkörperprobleme* (Friedr. Vieweg und Sohn, Braunschweig, Germany, 1962), Vol. 1, pp. 38–71.

[5] K. W. Böer, Phys. Rev. 139, A1949 (1965); K. W. Böer and W. E. Wilhelm, Phys. Status Solidi 3, 1704 (1964).

[6] J. B. Gunn, Solid State Commun. 1, 88 (1963); in *Proceedings of the Symposium on Plasma Effects in Solids, Paris, 1964* (Academic Press Inc., New York, 1965), p. 199; R. G. Pratt and B. K. Ridley, Proc. Phys. Soc. (London) 81, 996 (1963); J. Phys. Chem. Sol. 26, 21 (1965).

[7] E. M. Conwell, Solid State Phys. Suppl. 9 (1967).

[8] H. Kiess and F. Stöckmann, Phys. Status Solidi 4, 117 (1964).

[9] C. Fischler-Hazoni and F. E. Williams, Phys. Rev. 139, A583 (1965).

[10] S. G. Kalashnikov, M. S. Kagan, and V. A. Vdovenkov, Fiz. Tekhn. Pol. 1, 116 (1967) [English transl.: Soviet Phys.—Semicond. 1, 88 (1967)]; N. G. Zhadanova, M. S. Kagan, and S. G. Kalashnikov, Fiz. Tverd. Tela 8, 788 (1966) [English transl.: Soviet Phys.—Solid State 8, 632 (1966)]; V. L. Bonch-Bruevich and S. G. Kalashnikov, Fiz. Tverd. Tela 7, 750 (1965) [English transl.: Soviet Phys.—Solid State 7, 599 (1965)].

[11] K. W. Böer and P. L. Quinn, Phys. Status Solidi 17, 307 (1966).

[12] G. Döhler, dissertation, Marburg, 1966 (unpublished); Phys. Status Solidi 19, 555 (1967).
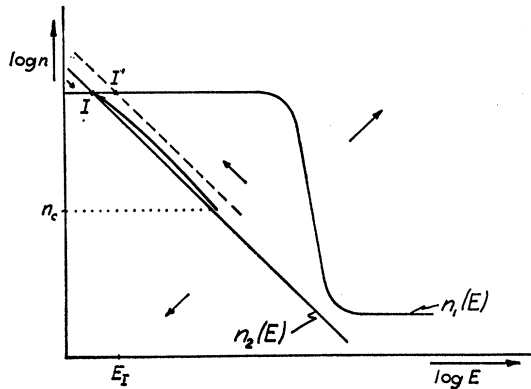
FIG. 1. Field of directions and solution curve projected in an $n$-$E$ plane for low applied voltages (barrier contact case); $n_c$ is the electron density at the cathode.



FIG. 3. Current-voltage characteristic. Points 1–7 correspond to the field distributions 1–7 in Fig. 2.

in agreement with experimental observations. (See Refs. 2, 5, and 11.) This is most easily seen in an analysis using the field of directions in the $n$-$E$ plane with the help of two auxiliary curves, $n_1(E)$ and $n_2(E)$, for which $\rho(x) \equiv 0$ and $j \equiv en\mu E$, respectively. These two curves divide the $n$-$E$ plane into regions of different direction of the projection of the solution curves. These regions and their respective field of direction are indicated by small arrows in Fig. 1.

The carrier density at the cathode is given by the work function and designated as $n_c$ in Fig. 1. [We shall discuss only blocking contacts $[n_c < n_1(E=0)]$; injecting contacts do not give cathode-adjacent high-field domains as experimentally observed.] The field at the cathode can then approximately be determined from Fig. 1, since under conditions valid for CdS and negligible hole contribution, the solution curve must start at $n_c$ between $n_2(E)$ and $n_1(E)$. This is the only range available for $E$ at the cathode resulting in a solution which can approach the singular point I' ($x$ increases from cathode towards anode). The heavy arrow given in Fig. 1 indicates a possible solution (disregarding the actual situation at the anode). Curve 1 in Fig. 2 repre-
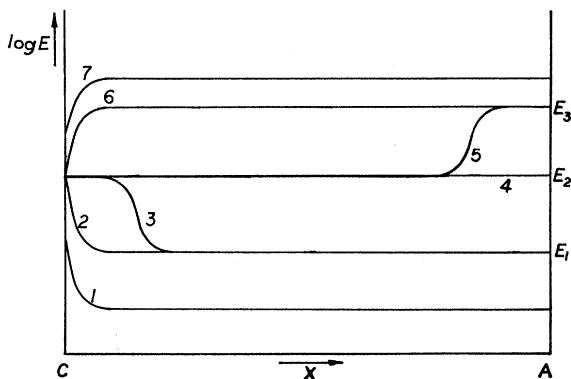
sents the corresponding field distribution. The fact that the average field in the crystal must be equal to the applied voltage divided by the electrode distance indicates that the current must be lower (point 1 in Fig. 3) than the "Ohmic current" (dashed line in Figure 3) for a completely homogeneous carrier density (singular point I' in Fig. 1). Hence the solution curve for the inhomogeneous case must extend below $E_{I'}$, close to the singular point I'.

With increasing applied voltage, the current increases [$n_2(E)$ is shifted upwards] until, in the region of negative differential conductivity, a second singular point (II) appears and approaches $n_c$ (see Fig. 4). The solution has the form a in Fig. 4 and is represented by curve 2 in Fig. 2 and by point 2 in Fig. 3.

With further increasing voltage, the current cannot readily increase. Only a very slight shift forces the solution curve, which must start at $n_c$, to start closer to the singular point II, i.e., to remain very close to $E_{II}$ for a longer distance $x$. Thus the solution curve, although having about the same form as II in Fig. 4, changes its general character as seen in Fig. 2, curve 3 (it becomes steplike). A numerical analysis[5] shows that the change from a field of about $E_{II}$ to a field of about $E_I$ takes



FIG. 2. Field distribution between cathode C and anode A for increasing applied voltage 1–7. The field values $E_I$, $E_{II}$, and $E_{III}$ correspond to the singular points I, II, and III in Fig. 4.
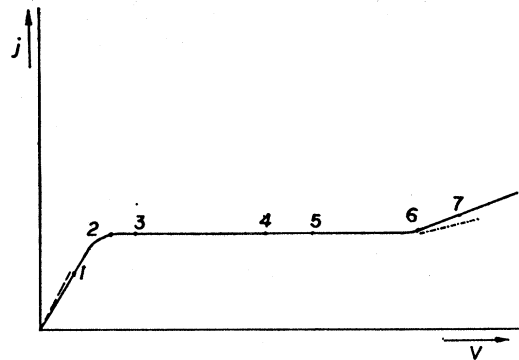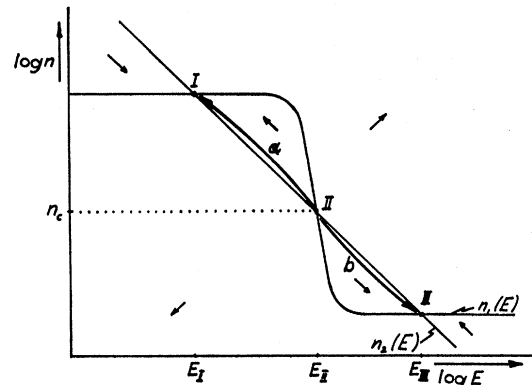


FIG. 4. Field of directions and projection of solution curves: a, typical for field distributions 3 and b, typical for field distributions 5 in Fig. 2.

place in a distance of the order of the Debye length, which is usually small as compared to the distance between the electrodes.[13] The current then saturates[14] (point 3 in Fig. 3).

With still further increasing applied voltages, $n_2(E)$ shifts up very slightly, the solution curves remain close to $E_{II}$ for a longer distance $(x)$, and the high-field domain increases in width. Finally, when $n_2(E)$ crosses $n_1(E)$ at $n_c$, a homogeneous solution (curve 4 in Fig. 2) is obtained—the trivial solution at the singular point: $n = n_c$ and $E = E_{II}$.

Increasing the applied voltage still more, a high-field domain adjacent to the anode should appear (solution type b in Fig. 4) with a shape given in curve 5 of Fig. 2. This domain should increase in width with further increasing voltage. The singular point II lies now just above $n_c$ and moves very slightly up with increasing voltage as long as the low-field domain close to the cathode has not completely disappeared; the current therefore remains saturated (see points 4 and 5 in Fig. 3). The current-voltage characteristic should in no way indicate the transition from a cathode- to an anode-high-field domain.

Finally, the low-field domain at the cathode disappears (curve 6 in Fig. 2), the current rises nearly proportionally to the applied voltage, and the solution curve becomes a type as given in Fig. 5 and correspondingly represented by curve 7 in Fig. 2. From a blocking contact behavior at low applied voltages (curve 1 in Fig. 2), the situation has changed to an injecting contact behavior at very high applied voltages. Because of carrier injection, the current is slightly higher than it would be for a homogeneous electron density $n_1(E_{III'})$ in the entire crystal[15] (represented by the dash-dot line in Fig. 3).

A general behavior as described above could be expected for a crystal with a cathode resulting in an electron density at the metal-CdS boundary lying between $n_H$ and $n_L$ (see Fig. 5), and having no moving field domains.

Measurement of the width of a high-field domain at the cathode (type 3 in Fig. 2) at different applied voltages gives the possibility to experimentally determine the fields $E_I$ and $E_{II}$, using the approximation
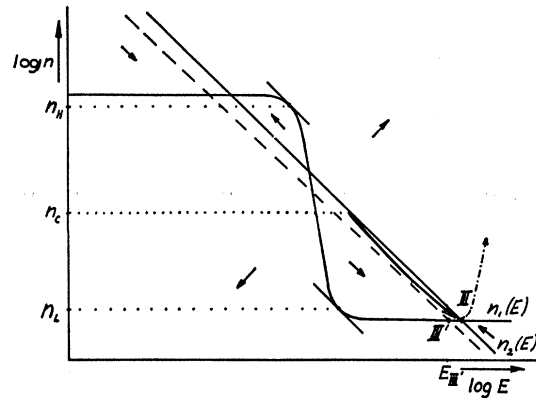
$$E_{II}l + E_I(L-l) = V, \qquad (2)$$



FIG. 5. Field of directions with projection of solution curve for high applied voltages (injection case). The dash-dot curve indicates a possible continuation of the solution curve towards the anode. (A metal with a work function similar to the cathode is assumed.) This part of the solution occupies only a very small fraction of the crystal.

where $l$ is the width of the high-field domain and $L$ is the distance between the electrodes. Similarly, the field value $E_{III}$ can be determined by measuring the width of a high-field domain at the anode (type 5 in Fig. 2) at different applied voltages.

Checking whether the domain width is a linear function of the applied voltage, and whether cathode- and anode-adjacent high-field domains yield approximately the same $E_{II}$ value, gives a possibility to check the applicability of the simplified theory to the observed experimental behavior.

With this technique one should be able to measure directly the work function between certain metals $(n_L < n_c < n_H)$ and CdS. Changing the optical excitation of CdS and determining $E_I$, $E_{II}$, and $E_{III}$ as a function of the light intensity gives direct information about the dependence of an "effective work function" on the optical excitation of a photoconductor. Investigations of this type will be published in a later paper.

## 4. EXPERIMENTAL RESULTS AND DISCUSSION

CdS:Cu,Al platelets, at higher applied voltages, showed a change from stationary to moving high-field domains and therefore could not be studied further in connection with the questions discussed in this paper.

CdS:Ag,Al platelets showed less tendency[16] to form moving domains, and cleaved small "stripes" from a platelet with an electrode distance of about 0.36 mm

---

[13] In a recent paper, V. L. Bonch-Bruevich [Phys. Status Solidi 23, 761 (1967)] discussed certain field inhomogeneities in "very short" crystals, or for "discontinuous solutions" in obviously inhomogeneous crystals. This discussion does not apply to macroscopic domains as investigated here and in Refs. 1–12. In order to obtain domain-shaped solutions with domain lengths long compared to the Debye length and a ratio of electric field in the high- and low-field regions of at least a factor of 4, as observed, one must leave the vicinity of the nodal point (singular point II in this paper). The solution has to extend at least from the vicinity of the nodal point to the vicinity of either saddle point (I or III).

[14] A very slight increase of the current with increasing voltage is expected according to the slight shift of $n_2(E)$.

[15] III' would be the singular point for such a homogeneous solution.

[16] Longer crystals cleaved from the same platelet show transitions from stationary to free-moving domains with increasing applied voltage, indicating that the stationary domain is not caused by structural defects of the crystal. This transition between stationary and moving domains is experimentally observed in the saturation range above a critical voltage, which, for a given doping, depends on optical excitation, temperature, and contact conditions (contact material and application). The reasons for a transition between stationary domains at lower applied voltages and moving domains above the critical voltage are not yet understood. A more detailed study of these transitions will be presented in a later paper.
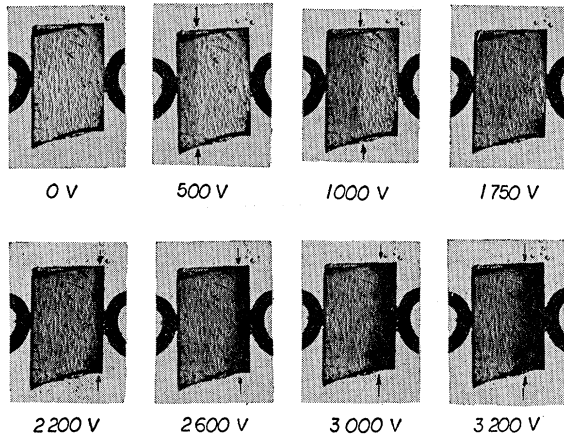
FIG. 6. Photographs of the CdS crystals at the given applied voltages (cathode at left side) in monochromatic light at the band edge, indicating high-field domains by increased darkening due to the Franz-Keldysh shift of the absorption edge. Arrows indicate boundary between high- and low-field region.

were suitable for investigating *stationary* domains up to a range where the anode-adjacent high-field domains extended over a major portion of the crystal for applied voltages below 3000 V. In order to avoid discharges across the surface, the crystal and the electrodes were imbedded in an epoxy layer.

The set of photographs given in Fig. 6 shows the high- and low-field domains (the cathode-adjacent high-field domains are less distinguishable). For easier identification, the boundary is indicated by two arrows adjacent to the crystal. The boundary is not completely parallel to the electrodes, which might be due to inhomogeneous doping or slight changes of $n_c$ along the cathode.

Figure 7 shows the width of the domain as a function of the applied voltage for cathode-adjacent (curve A) and anode-adjacent (curve B) high-field domains. (The width is determined at the narrowest part of the
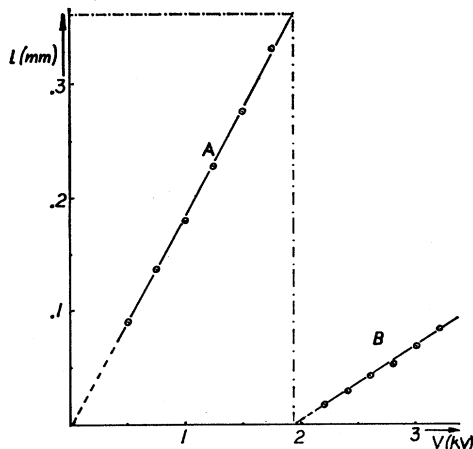


FIG. 7. Width ($l$) of the high-field domain as a function of the applied voltage: A, high-field domain adjacent to the cathode; B, high-field domain adjacent to the anode.
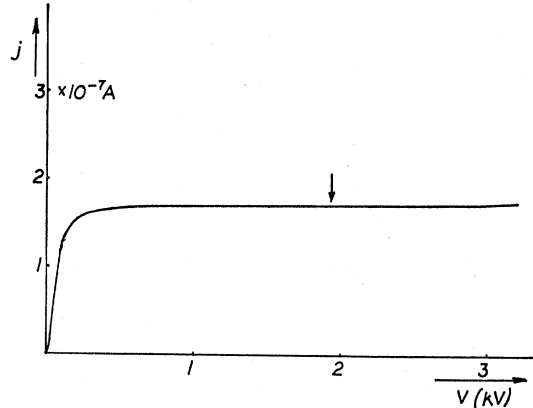


FIG. 8. Measured current-voltage characteristic for the crystal analyzed in Figs. 6 and 7.

domain.) It can be seen that the width of the high-field domains is reasonably well a linear function of the applied voltage. (For very thin domains, some deviations from the linear law are observed and indicate that the domains are not yet fully developed.)

Using Eq. (2) one calculates from the intersection with the abscissa[17] and the slope of curve A (Fig. 7) $E_I \simeq 1$ and $E_{II} \simeq 54$ kV/cm, and from curve B one obtains $E_{II} \simeq 54$ and $E_{III} = 205$ kV/cm.

The excellent agreement of $E_{II}$ and the observed current saturation which shows, as expected, no marked change at the transition voltage (arrow in Fig. 8) between cathode- and anode-adjacent high-field domain, indicates the applicability of the theory.

With the voltage applied in the opposite direction, the formation of a stationary domain and current saturation are also observed. The saturation current is lower by a factor of 4 and the field $E_{II}$ is higher than reported
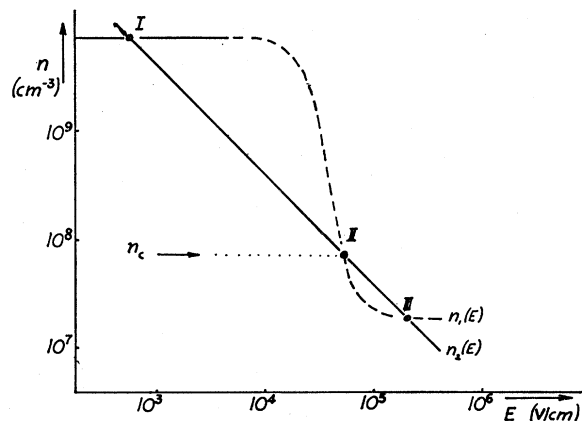


FIG. 9. $n_2(E)$ with measured singular points I, II, and III, measured $n_c$, and a suggested $n_1(E)$ curve.

[17] In longer crystals and crystals with an Ohmic contact, $E_I$ can be determined with much higher accuracy and was obtained for similar conditions as $E_I = 600$ V/cm, which agrees well with the value given here. In Fig. 9, therefore, the more accurate value is plotted.

above, in agreement with the model proposed. The electron concentration at the cathode is lower than for the opposite electrode[18] when used as a cathode, indicating that for the results reported in this paper, $n_c > n_L$.

It is concluded that this crystal (doped with Ag and Al and having a bulk electron density of $8 \times 10^9$ cm$^{-3}$ at low fields) with evaporated Au electrodes has a boundary electron density of $n_c = 8 \times 10^7$ cm$^{-3}$, and shows a negative differential conductivity range with a slope steeper than $-1$ at about $E_{II} = 55$ kV/cm. This value of $n_c$ yields an effective work function $\psi_{\text{Au,CdS:Ag,Al}}$ (505 m$\mu$, $10^{12}$ photon/cm$^2$ sec) $= 0.42$ eV and was obtained for a temperature of $-65°$C and an optical excitation of $\sim 10^{12}$ photon/cm$^2$ sec, with a band width of 10 m$\mu$ centered at 505 m$\mu$. The bulk electron density at high fields is decreased by more than two orders of magnitude, presumably by field quenching, and is about $2 \times 10^7$ cm$^{-3}$ at $E_{III} \simeq 205$ kV/cm. The quasineutrality

curve $n_1(E)$ might[19] have a form as given in Fig. 9. The experimentally obtained values are indicated by circles.

An experimental determination of a wider range of the $n_1(E)$ curve is currently under way, using as a virtual cathode with an easily variable boundary density a shadow region parallel to the cathode, and a variable low-intensity optical excitation in the shadow region. Results of these investigations are reported in Ref. 20.

### ACKNOWLEDGMENTS

---

[18] The electrodes were evaporated at different runs; the electrode with lower $n_c$ was less homogeneous and caused a less homogeneous cathode adjacent high-field domain.

[19] The Franz-Keldysh-effect band-edge shift tends to flatten the $n_1$ curve somewhat since the photoconductivity increases with increasing field due to increased absorption of the monochromatic optical excitation (for assumed homogeneous excitation in direction of the light beam). For very-high-field domains, inhomogeneous excitation in the direction of the light beam might influence the current and field distribution. These effects are neglected here.
[20] K. W. Boer, G. Doehler, G. A. Dussel, and P. Voss, Phys. Rev. **169**, 700 (1968).

---

# Photoelectronic Properties of ZnSe Crystals*†

GERALD B. STRINGFELLOW‡ AND RICHARD H. BUBE

*Department of Materials Science, Stanford University, Stanford, California*

(Received 9 February 1968)

The photoelectronic properties of $p$-type ZnSe:Cu and of $n$-type self-activated ZnSe(SA) have been investigated in single crystals. Results for ZnSe:Cu may be described by a multivalent-copper-impurity model in which Cu$^+$ and Cu$^{+2}$ ions substituting on the Zn sublattice are responsible for the red and green luminescence bands, respectively. The green luminescence emission (2.34 eV) is from the conduction band to the empty Cu$_{Zn}^x$ center. One of the red emission bands (1.97 eV) is from the conduction band to the empty Cu$_{Zn}'$ center; a second red band (1.95 eV) is from a shallow level near the conduction band to the empty Cu$_{Zn}'$ center. The Cu$_{Zn}'$ center is also the major sensitizing center for $n$-type photoconductivity in $p$-type ZnSe:Cu, and it is the dominant acceptor center controlling $p$-type conductivity. Optical absorption in the infrared is due to an internal transition within the Cu$_{Zn}^x$, which has an (Ar) $3d^9$ electronic configuration, plus a transition from the valence band to the empty Cu$_{Zn}'$ center. Several annealing and impurity-incorporation experiments performed on ZnSe:Cu support this model for the Cu luminescence centers. The sensitizing center for $n$-type photoconductivity in $n$-type ZnSe(SA) is not the same as that associated with Cu$_{Zn}'$ in $p$-type ZnSe:Cu; it lies closer to the valence band and has a capture cross section for electrons $10^{-3}$ that of the Cu$_{Zn}'$ sensitizing center.

## INTRODUCTION

T HE purpose of this investigation has been to examine the luminescence, photoconductivity, and optical absorption of single crystals of ZnSe:Cu and of self-activated ZnSe(SA), well characterized with

respect to impurities and structure. A major portion of the investigation has been devoted to $p$-type ZnSe:Cu crystals, but a number of measurements have been made for comparison on $n$-type ZnSe(SA).

Copper impurity has long played a central role in the photoelectronic properties of many II-VI compounds. Copper, substituting on the zinc sublattice in ZnSe is an acceptor. In the chemically neutral state, copper has an electronic structure of (Ar)$3d^{10}4s^1$; copper substituted for zinc, Cu$_{Zn}^x$, therefore has the (Ar) $3d^9$ configuration. If the ionic approximation were perfectly valid and the $3d$ electrons were shielded from the valence and conduction band wave functions, the
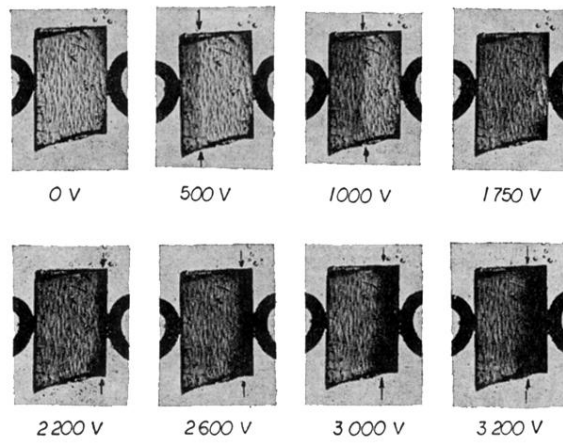
---

FIG. 6. Photographs of the CdS crystals at the given applied voltages (cathode at left side) in monochromatic light at the band edge, indicating high-field domains by increased darkening due to the Franz-Keldysh shift of the absorption edge. Arrows indicate boundary between high- and low-field region.